



Contents lists available at ScienceDirect

Bioorganic & Medicinal Chemistry Letters

journal homepage: www.elsevier.com/locate/bmcl

Synthesis and evaluation of new 2-chloro-4-aminopyrimidine and 2,6-dimethyl-4-aminopyrimidine derivatives as tubulin polymerization inhibitors

Shaoyu Xu^a, Baijiao An^b, Yuxin Li^c, Xunbang Luo^a, Xingshu Li^{b,*}, Xian Jia^{a,*}

^aSchool of Pharmaceutical Engineering, Shenyang Pharmaceutical University, Shenyang 110016, China

^bSchool of Pharmaceutical Sciences, Sun Yat-sen University, Guangzhou 510006, China

^cSchool of Life Sciences & Biopharmaceutical Sciences, Shenyang Pharmaceutical University, Shenyang 110016, China

ARTICLE INFO

Article history:

Received 9 February 2018

Revised 7 April 2018

Accepted 11 April 2018

Available online xxx

Keywords:

Tubulin polymerization inhibitors

Design and synthesis

Antiproliferative activity

Mechanism

ABSTRACT

Eighteen new 2-chloro-4-aminopyrimidine and 2,6-dimethyl-4-aminopyrimidine derivatives were synthesized and evaluated as tubulin polymerization inhibitor for the treatment of cancer. Among them, compounds **10**, **17**, **20** and **21** exhibited potent antiproliferative activities against five human cancer cell lines. Microtubule dynamics assay showed that compound **17** could effectively inhibit tubulin polymerization. Molecular docking studies were also carried out to understand the binding pattern. Further mechanism studies revealed that **17** could induce G2/M phase arrest, disrupt the organization of the cellular microtubule network and induce cell apoptosis and mitochondrial dysfunction.

© 2018 Elsevier Ltd. All rights reserved.

Tubulin-microtubule systems play a critical role in cell growth, division, and cytoskeletal organization as well as being implicated in motility, shape, and intracellular transport.¹ These features make microtubules an attractive target for cancer therapy.^{2,3} A number of natural compounds, such as paclitaxel, epothilone, vinblastine, combretastatin A-4 (CA-4), dolastatin and colchicine, which interfere the dynamics of tubulin polymerization and depolymerization, have been marketed or is undergoing clinical research.⁴ Among them, taxanes and vinca alkaloids have been proved to be effective in the treatment of diverse human cancers.⁵ In the last decades, the design and synthesis of structurally diverse tubulin polymerization and depolymerization inhibitors were also flourishing. For instance, MPC-6827 (A)^{6–9} and its analogues (B),¹⁰ 4-arylcoumarin analogue (C),^{11,12} and Se-aspirin analogue (D)¹³ exhibited potent anticancer activities against a broad-spectrum of human cancer cell lines (Fig. 1).

In our study to search for new structural compounds as anti-cancer agents, we have developed several series of compounds, such as indole-chalcone derivatives, selenium-containing isocombretastatins and phenstatins derivatives, which had been proved to exert their effective antitumor activity through microtubule destabilization *in vitro* and *in vivo*.^{14,15} Inspired by MPC-6827

(which has reached phase II trials for the treatment of recurrent glioblastoma), we expected to search for new more effective anti-tumor lead molecules. Starting from the diversity of molecular structure screening, we decided to make an attempt to synthesize and evaluate the 2-chloro-4-aminopyrimidine and 2,6-dimethyl-4-aminopyrimidine derivatives that have the similar pharmacophores to MPC-6827 but smaller molecular weight.

The synthetic method of new 2,4-dichloropyrimidine derivatives (**3a-3c**) is shown in scheme 1. The reaction of 2,4-dichloropyrimidine with 4-methoxy-*N*-methylaniline or its fluorine, chlorine derivatives (**2a-2c**) in 2-propanol at room temperature provides the target compounds **3a-3c** in a good yields. 4-Fluoro-3-nitroaniline (**4**) was *N*-methylated by reacting with paraformaldehyde in MeONa-MeOH solution and then sodium borohydride to afford 4-methoxy-*N*-methyl-3-nitroaniline (**5**), which reacted with 2,4-dichloropyrimidine to give compound **6**. Compound **10** is synthesized via a four-step procedure. First, the hydroxyl of 2-methoxy-5-nitrophenol (**7**) was protected by MOM, and then hydrogenated in the presence of palladium/C to give intermediate **8**, followed by a methylation of amino group to give compound **9**, finally, **9** reacted with 2,4-dichloropyrimidine to give the target compound **10**.

Scheme 2 listed the synthetic route of compounds containing 4-methoxy-3-bromoalkoxy or 4-methoxy-3-cyanoselenoalkoxy group at anilino moiety. The reaction of compound **10** with dibro-

* Corresponding authors.

E-mail addresses: lixsh@mail.sysu.edu.cn (X. Li), jiaxian@syphu.edu.cn (X. Jia).

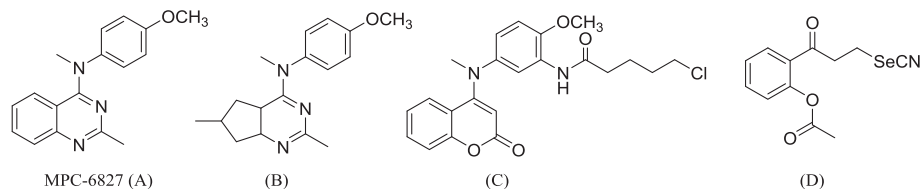
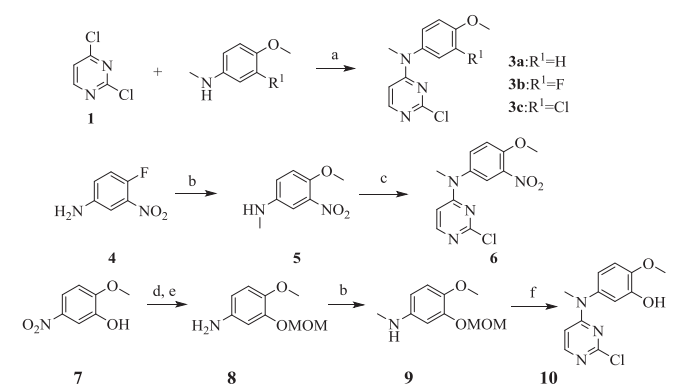


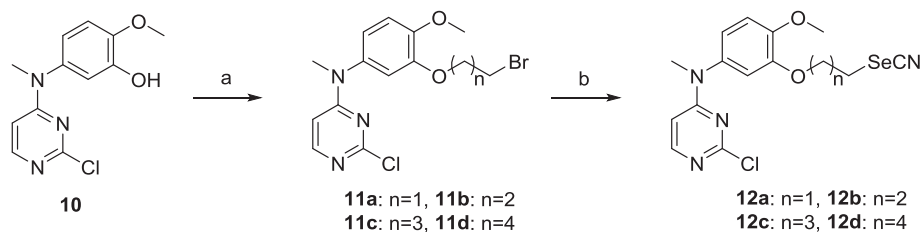
Fig. 1. Some reported tubulin polymerization and depolymerization inhibitors.

moalkanes in the presence of potassium carbonate gave **11a–11d**, which reacted with potassium cyanide to give compound **12a–12d**.

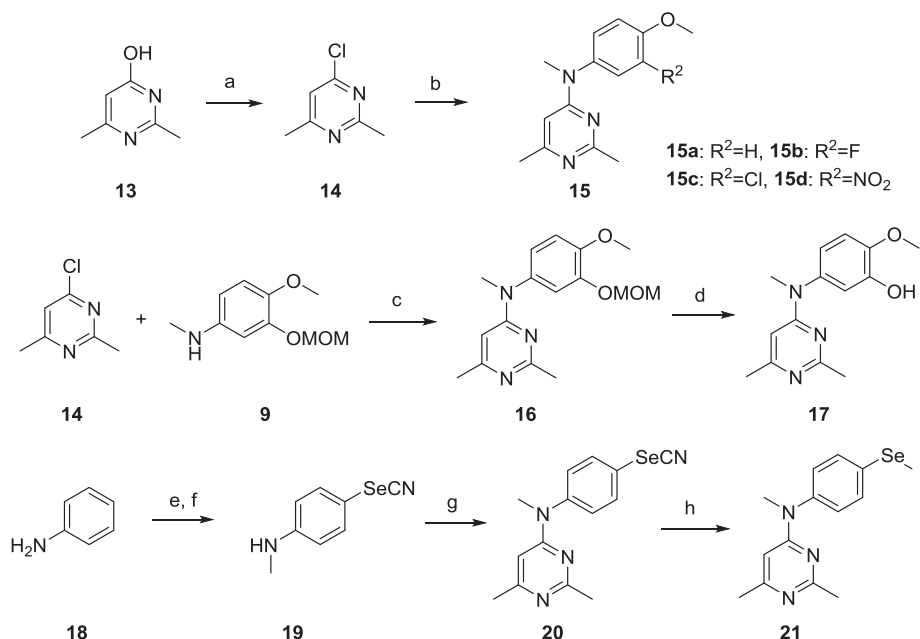
The synthetic routes to 2,4-dimethylpyrimidine derivatives (**15**, **17**, **20** and **21**) are shown in Scheme 3. The reaction of 2,6-dimethylpyrimidin-4-ol (**13**) with phosphoryl trichloride gave 4-chloro-2,6-dimethylpyrimidine (**14**), which reacted with the corresponding anilines to provide the target compounds **15a–15d**. The reaction of compound **14** with **9** afforded compound **16**, followed by a deprotection in the presence of hydrogen chloride in ethyl acetate to afford the target compound **17**. Selenocyanato-containing compound **20** was prepared through the reaction of **14** with 4-selenocyanatoaniline (**19**), which was obtained by nitrogen methylation of aniline followed by the reaction with malononitrile in the presence of selenium dioxide. The methylseleno derivative (**21**) was obtained by the reaction of **20** with sodium borohydride and methyl iodide.



Scheme 1. Reagents and conditions: a) isopropanol, r.t. b) (i) (CH₂O)_n, CH₃ONa, MeOH, r.t. (ii) NaBH₄, reflux. c) 2,4-dichloropyrimidine, isopropanol, r.t. d) MOMCl, DIPEA, DCM, 0 °C. e) Pd/C, H₂, MeOH, r.t. f) 2,4-dichloropyrimidine, HCl, isopropanol, r.t.



Scheme 2. Reagents and conditions: a) K₂CO₃, Br(CH₂)_nBr, CH₃CN, reflux. b) KSeCN, CH₃CN, reflux.

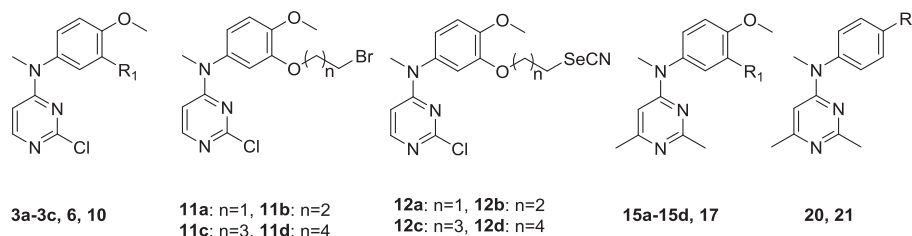


Scheme 3. Reagents and conditions: a) POCl₃, toluene, reflux. b) **2** or **5**, isopropanol, r.t. c) isopropanol, r.t. d) HCl, isopropanol, r.t. e) (i) (CH₂O)_n, CH₃ONa, MeOH, r.t. (ii) NaBH₄, reflux. f) malononitrile, SeO₂, DMSO, r.t. g) **14**, isopropanol, r.t. h) NaBH₄, CH₃I, ethanol, r.t.

In vitro antiproliferative activity of the compounds **3a-3c**, **6**, **10**, **11a-11d**, **12a-12d**, **15a-15d**, **17**, **20**, **21** was evaluated against five types of human cancer cell lines including A549 (non-small cell lung carcinoma), Hela (human epithelial cervical cancer cell line), HCT-116 (human colon cancer cell line), HEPG2 (Human hepatoma carcinoma cells) and MDAMB231 (Human breast cancer cells) employing MTT assay and the results were summarized in Table 1. Compounds **3a-3c**, 4-OCH₃, 3-F/4-OCH₃, or 3-Cl/4-OCH₃ substitution at the aniline moiety, exhibited good antiproliferative activities with the IC₅₀ values range from 0.611 to 2.815 μM against five cancer cell lines. Nitro group seems not favorable for the activity, compound **6**, with 3-NO₂/4-OCH₃ at the same position, pro-

vided relatively poor activities compared with **3a-3c**. However, compound **10**, with hydroxyl at 3-position, exhibited much better activity with IC₅₀ values range from 0.096 to 0.833 μM on the five human cancer cell lines, respectively. **11a-11d** (3-bromoalkoxy-containing derivatives) and **12a-12d** (selenocyanato-containing derivatives), exhibited lower activities than that of **10**, the parent compound. Possibly due to the stereo effects on the antitumor activity, *N*,2,6-trimethylpyrimidin-4-amine derivatives (**15**, **17**, **20** and **21**) exhibited better antiproliferative activities in some cases compared with the *N*-methyl-2-chloropyrimidin-4-amine series (**3**, **6**, **10**, **11**, **12**). Among them, compound **17**, with 3-OH/4-OCH₃ substitution at the aniline moiety, showed the best

Table 1

Antiproliferative activities of **3a-3c**, **6**, **10**, **11a-11d**, **12a-12d**, **15a-15d**, **17**, **20**, **21** against Human Cancer Cell Lines.^a

Comp.	R ₁	R ₂	IC ₅₀ (μM) ^b				
			A549	Hela	HCT116	HepG2	MDAMB231
3a	H	–	0.611 ± 0.034	0.917 ± 0.048	1.460 ± 0.096	2.122 ± 0.082	2.815 ± 0.036
3b	F	–	0.651 ± 0.011	0.241 ± 0.015	0.914 ± 0.015	0.844 ± 0.048	1.275 ± 0.080
3c	Cl	–	0.621 ± 0.016	0.517 ± 0.0139	1.172 ± 0.017	2.628 ± 0.073	1.376 ± 0.058
6	NO ₂	–	3.784 ± 0.0855	4.725 ± 0.0634	4.701 ± 0.0967	6.122 ± 0.0152	8.116 ± 0.0779
10	OH	–	0.381 ± 0.010	0.096 ± 0.009	0.422 ± 0.038	0.464 ± 0.022	0.833 ± 0.056
11a	–	–	4.638 ± 0.0685	3.307 ± 0.0416	5.674 ± 0.125	7.724 ± 0.197	6.62 ± 0.0468
11b	–	–	0.862 ± 0.0323	0.307 ± 0.009	1.97 ± 0.0381	1.237 ± 0.0592	1.277 ± 0.0975
11c	–	–	0.591 ± 0.0616	0.307 ± 0.0038	1.138 ± 0.0779	0.168 ± 0.0104	0.992 ± 0.0417
11d	–	–	9.715 ± 0.174	7.085 ± 0.0971	>10	>10	>10
12a	–	–	0.463 ± 0.0124	0.436 ± 0.0082	1.221 ± 0.0157	1.667 ± 0.0446	2.75 ± 0.0135
12b	–	–	3.708 ± 0.0104	4.714 ± 0.0408	3.923 ± 0.0104	5.152 ± 0.0226	1.485 ± 0.0317
12c	–	–	>10	>10	>10	>10	>10
12d	–	–	>10	>10	>10	>10	>10
15a	H	–	0.277 ± 0.0282	0.322 ± 0.0208	1.318 ± 0.0432	0.824 ± 0.0114	3.646 ± 0.0512
15b	F	–	0.632 ± 0.0141	0.471 ± 0.0107	0.584 ± 0.0127	2.055 ± 0.124	2.785 ± 0.0957
15c	Cl	–	0.780 ± 0.025	0.316 ± 0.098	1.189 ± 0.039	0.787 ± 0.0177	1.901 ± 0.0475
15d	NO ₂	–	3.271 ± 0.019	3.72 ± 0.085	4.674 ± 0.094	2.985 ± 0.055	3.441 ± 0.039
17	OH	–	0.113 ± 0.004	0.093 ± 0.008	0.126 ± 0.009	0.112 ± 0.025	1.101 ± 0.086
20	–	SeCN	0.207 ± 0.008	0.252 ± 0.008	0.245 ± 0.017	0.155 ± 0.0141	0.614 ± 0.009
21	–	SeMe	0.218 ± 0.006	0.138 ± 0.009	0.465 ± 0.012	0.198 ± 0.018	0.321 ± 0.084
MPC-6827	–	–	0.004 ± 0.001	0.006 ± 0.001	0.005 ± 0.001	0.005 ± 0.002	0.008 ± 0.001

^a Cell lines were treated with compounds for 48 h. Cell viability was measured by MTT assay as described in the Experimental Section.

^b IC₅₀ values are indicated as the mean ± SD (standard error) of at least three independent experiments.

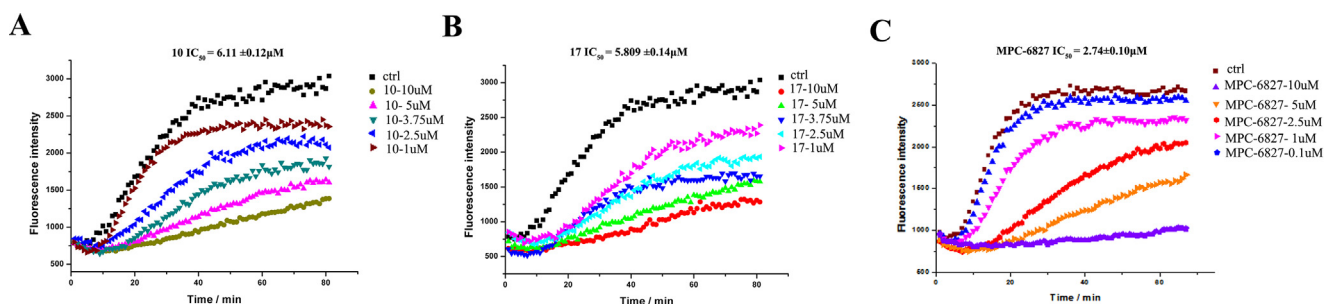


Fig. 2. Tubulin polymerization inhibition activity of **10**, **17**, MPC-6827. The tubulin polymerization assay was performed according to the method described by Bonne, D. et al. with appropriate modification. **16–18** Purified tubulin protein at 10 μM in a reaction buffer was incubated at 37 °C in the absence (control) or presence of **10**, **17**, MPC-6827 at the indicated concentrations. Polymerizations are followed by an increase in fluorescence emission at 410 nm over a 60 min period at 37 °C (excitation wavelength was 340 nm). The experiments were performed at least three times, and the results of the representative experiments were shown.

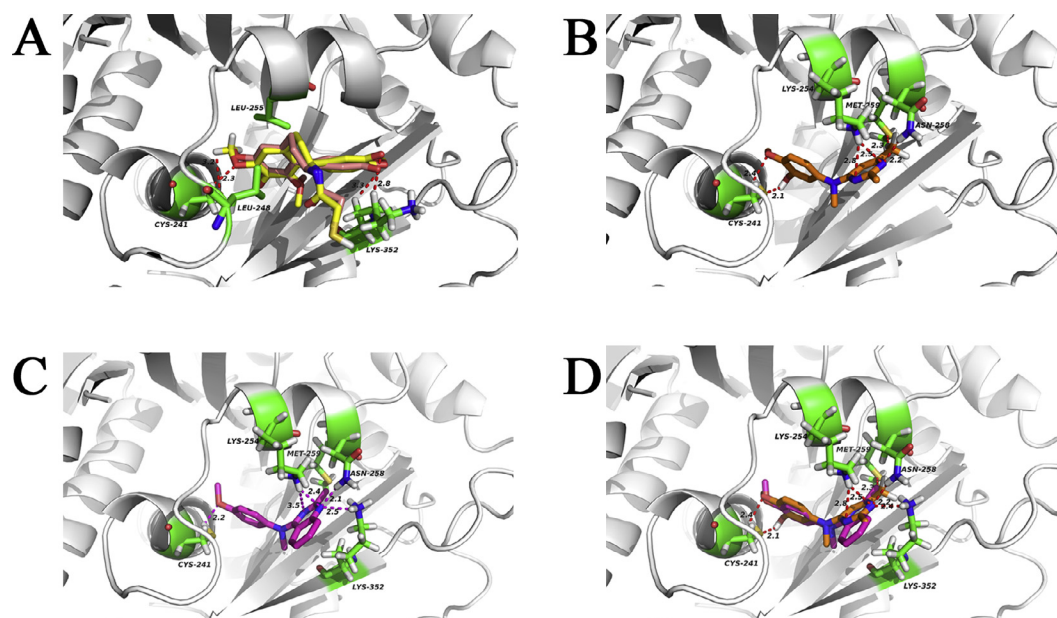


Fig. 3. Molecular docking results of compounds (A) Colchicine (original X-ray structure of the colchicine was shown in pink, docked conformation of the colchicine was shown in yellow) (B) **17** (shown in orange) (C) MPC-6827 (shown in purple) (D) MPC-6827 (shown in purple) and **17** (shown in orange) with colchicine binding site (PDB code: 1SA0).

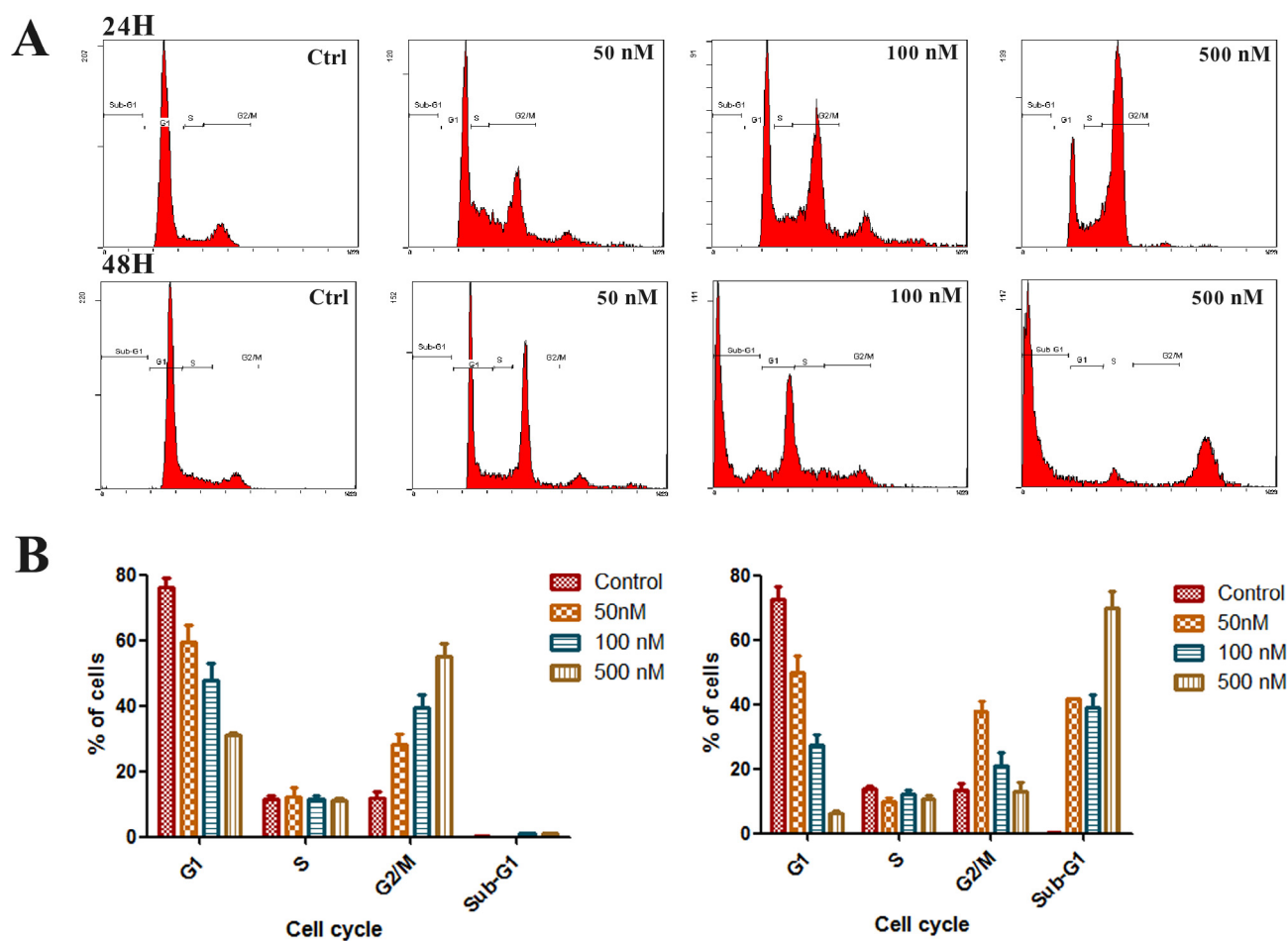


Fig. 4. Cell cycle arrest effect of **17**. (A) The HeLa cells were treated with compound **17** (50, 100 and 500 nM) or DMSO (0.01%) for 24 h or 48 h. (B) Quantitative analysis of the percentage of cells in each cell cycle phase were analyzed by EXPO32 ADC analysis software. The experiments were performed three times, and the results of representative experiments were shown.

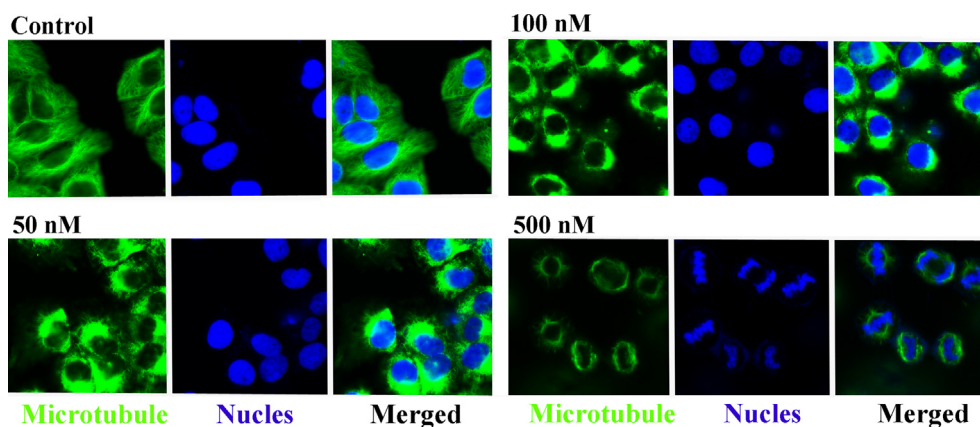


Fig. 5. Compound **17** disrupted the organization of the cellular microtubule network at indicated concentrations. The detection of the fixed and stained HeLa cells was performed with an LSM 570 laser confocal microscope (Carl Zeiss, Germany). The experiments were performed three times.

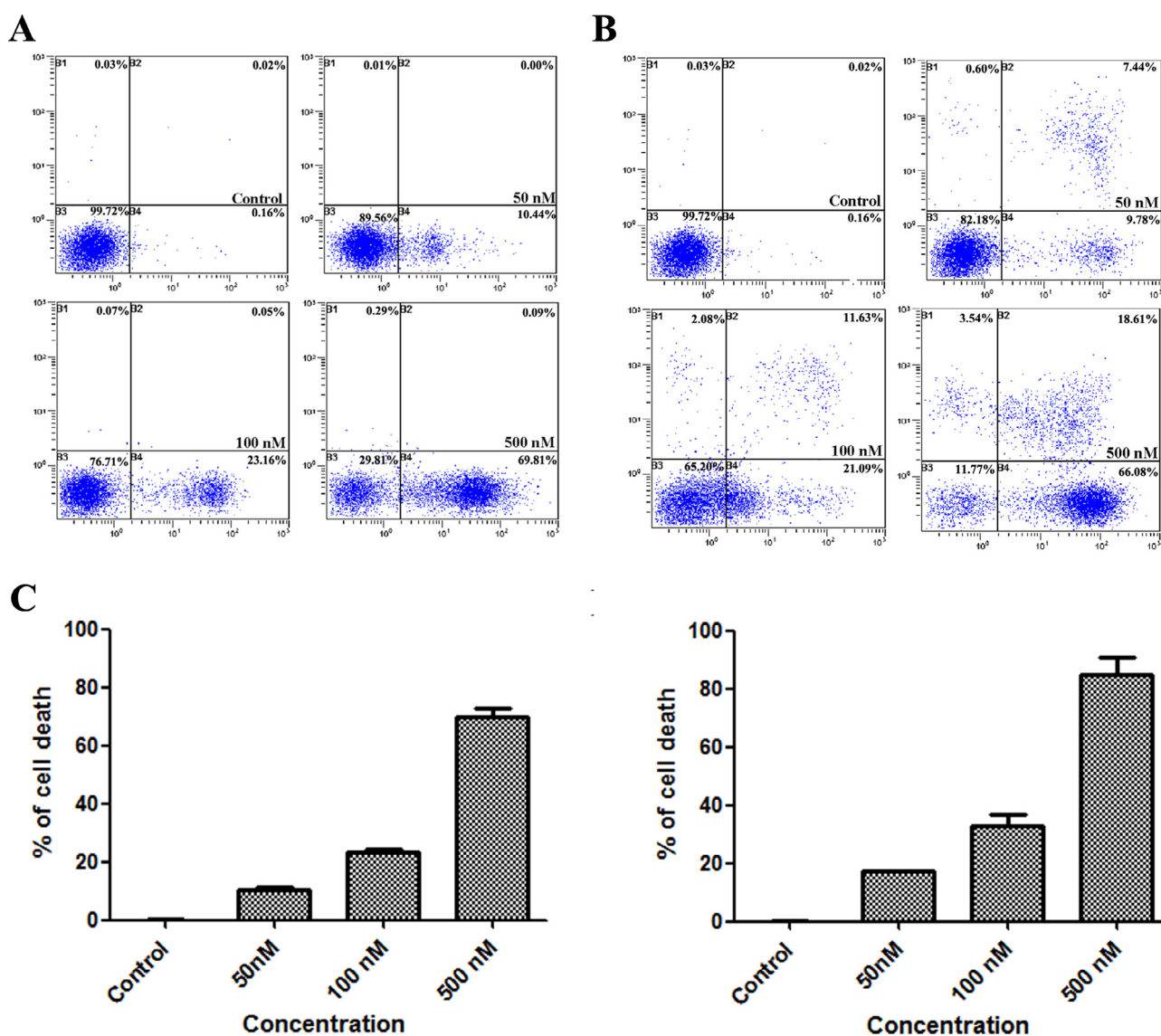


Fig. 6. Effect of **17** on cell apoptosis progression and the mitochondrial membrane potential of HeLa cells. Induction of apoptosis in the cultured HeLa cells upon treatment with compound **17** (0.05, 0.10 and 0.50 μ M) or DMSO (0.01%) for 48 h (A) or 72 h (B), the cell apoptosis profile was analyzed by flow cytometry. (C) Quantitative analysis of the percentage of death cells were analyzed by EXPO32 ADC analysis software. The experiments were performed at least three times, and the results of the representative experiments were shown.

activity with the IC₅₀ values from 0.093 to 1.101 μM. Interesting, the pharmacophore (3-OH/4-OCH₃) are also found in other tubulin inhibitors such as colchicin and combretastatin A4.

To elucidate whether these compounds target the tubulin-microtubule system, compounds **10** and **17**, which showed better anti-proliferative activity in the initial cytotoxicity screening, was chosen to test the inhibitory effect on microtubule assembly in vitro, with MPC-6827 as the reference compound. As shown in Fig. 2, the increased fluorescence intensity with time of the purified and unpolymerized tubulin control samples indicated that tubulin polymerization had occurred. The IC₅₀ of compounds **10**, **17** and MPC-6827 were 6.11 ± 0.12, 5.809 ± 0.14, and 2.74 ± 0.10 μM, respectively.

Compound **17** displayed good antiproliferative activity and effective tubulin polymerization inhibition, therefore we decided to perform a molecular docking study to investigate the potential binding site of compound **17** to colchicine binding site of tubulin-microtubule system. Docking studies with the suite AutoDock Vina predicted **17** to bind in an orientation analogous to colchicine. As shown in Fig. 3A, colchicine could be re-docked in the colchicine binding site in a similar conformation to the X-ray structure of the colchicine (PDB code: 1SA0), which indicated the reliability of our docking method. Then we applied this docking method to **17** (Fig. 3B). The docking results showed that **17** occupied the binding cavity of tubulin. Fig. 3C and D provided further evidence that compound **17** could bind the same site as MPC-6827. The binding free energy of compound **17** and MPC-6827 inclusion complexes with protein obtained from AutoDock-Vina are -8.6 and -7.9 kcal mol⁻¹, respectively, which confirmed that **17**-protein complex is more stable than that of MPC-6827-protein.

Then the flow cytometry analysis was performed to study its effect on the cell cycle using human cervical carcinoma (Hela) cell. As indicated in Fig. 4, comparing with control, the tetraploid peaks (28.3%) increased when Hela cells were treated with **17** at 50 nM for 24 h, indicating **17** induced cell cycle arrest at the G2/M phase. The percentage of cells at the G2/M phase increased to 39.6% and 55.6% with the increase of **17** to 100, and 500 nM, respectively. When incubation time was extended to 48 h, tetra-

ploid peaks was still obvious at 50 nM (38.7%). However, when the cells were exposed at relatively high concentration of **17** (100 or 500 nM), most of the cells died and the G2/M phase almost disappeared; cell cycle arrest at the sub-G1 peak (a characteristic hypodiploid peak) was found to be the main peak, which indicated most cells underwent DNA fragment. These results are consistent with the performance of most tubulin inhibitors.

To study the morphological alterations of cancer cells caused by compound **17**, human cervical carcinoma (Hela) cells were exposed to different concentrations of **17** (0.05, 0.10 and 0.50 μM) for 24 h and then observed under an LSM 570 laser confocal microscope. As shown in Fig. 5, the integrity of the mitotic spindle and cellular microtubule network of the Hela cells was obvious in the control group. After treatment with **17** at the concentration of 0.050 μM, the spindle microtubule organization was significantly deranged. At 0.50 μM, the nucleus of the cells narrowed sharply and spindle microtubules were disorganized completely.

Subsequently, apoptosis was measured using propidium iodide (PI) and fluorescent immunolabeling of the protein annexin-V (V-FITC) by flow cytometry. When Hela cells were treated for 48 h with **17** at indicated concentrations, the Hela cells were harvested, stained with Annexin V-FITC and PI, and analyzed by flow cytometry. The results showed 10.44%, 23.21%, 69.90% and 0.18% of the early and late apoptosis cells at the concentrations of 0.05, 0.1 and 0.5 μM or DMSO (0.01%), respectively (Fig. 6A). When the incubation time was extended to 72 h (Fig. 6B), the early and late apoptosis cells increased to 17.22%, 32.72%, 84.69% and 0.18%, respectively. These results indicated that **17** induced cell apoptosis in a concentration- and time-dependent manner.

Mitochondria are highly dynamic organelles which play an important role in regulating the life and death of cells, and its dysfunction is closely related to apoptosis. To study the possible involvement of mitochondrial dysfunction in **17**-induced apoptosis of the cells, we performed the quantitative MMPs (mitochondrial transmembrane potential) assay with JC-1 staining. The change of MMP could be detected by flow cytometry analysis or a laser scanning confocal microscope. As shown in Fig. 7, when the Hela cells were exposed to the indicated concentrations (50, 100, and

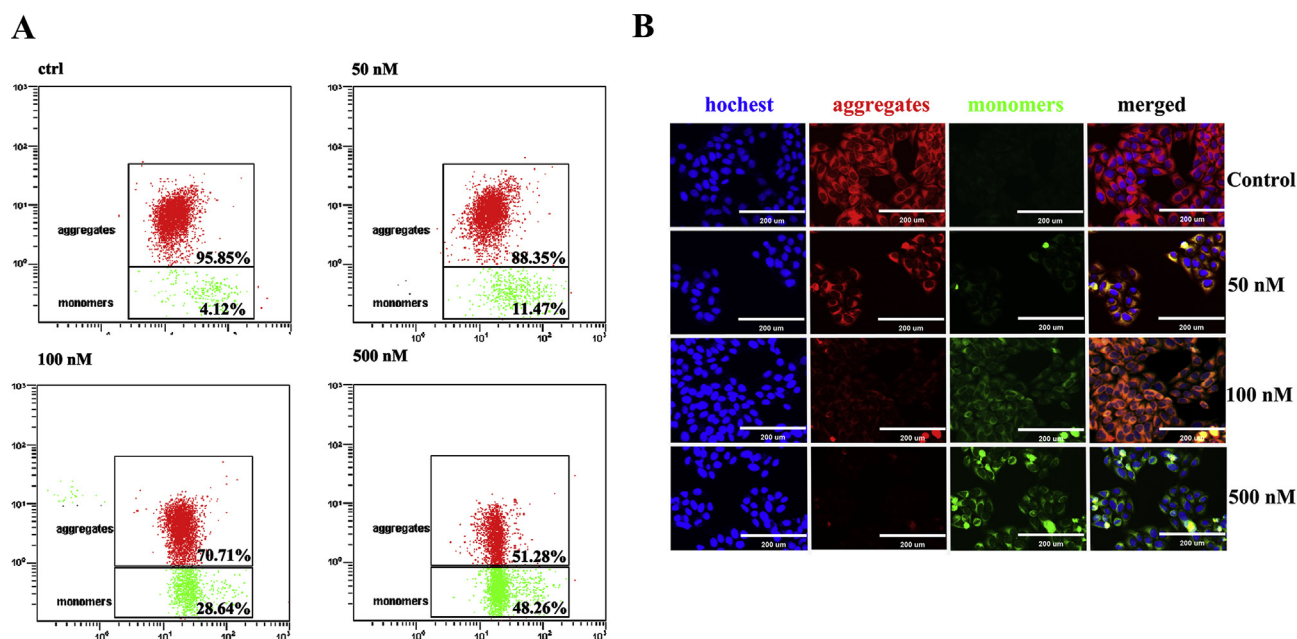


Fig. 7. The Hela cells were treated with **17** at the indicated concentration for 24 h, followed by incubation with the fluorescence probe JC-1 for 30 min. Then, the cells were analyzed by flow cytometry (A) or fluorescence microscopy (B). The experiments were performed at least three times, and the results of the representative experiments are shown.

500 nM) or DMSO (0.01%) for 24 h, a rapid collapse of MMP was detected as a consequence of the opening of the permeability transition pores that accumulate fluorescent dye from its red aggregated to green-monomeric forms (monomers: aggregates = 11.47:88.35; 28.64:70.71; 48.26:51.28, respectively). Taken together, **17** could induce mitochondrial dysfunction and eventually triggered apoptotic cell death.

In conclusion, we have developed a series of new 2-chloro-4-aminopyrimidine and 2,6-dimethyl-4-aminopyrimidine derivatives as tubulin polymerization inhibitors. Among them, compound **17** exhibited very good antiproliferative activity against five tested cancer cell lines with the IC₅₀ values from 0.093 to 1.101 μM. Mechanism study demonstrated that **17** could arrest cell-cycle progression, induce cell apoptosis and mitochondrial dysfunction. Moreover, **17** showed good tubulin polymerization inhibitory activity with the IC₅₀ value of 5.809 μM. The further *in vivo* anti-tumor evaluations on **17** are still in progress.

A. Supplementary data

Supplementary data associated with this article can be found, in the online version, at <https://doi.org/10.1016/j.bmcl.2018.04.026>. These data include MOL files and InChIKeys of the most important compounds described in this article.

References

- Downing KH, Nogales E. Tubulin and microtubule structure. *Curr Opin Cell Biol.* 1998;10:16–22.
- Horio T, Murata T. The role of dynamic instability in microtubule organization. *Front Plant Sci.* 2014;5:511.
- Pellegrini F, Budman DR. Review: tubulin function, action of antitubulin drugs, and new drug development. *Cancer Invest.* 2005;23:264–273.
- Hamel E. Antimitotic natural products and their interactions with tubulin. *Med Res Rev.* 1996;16:207–231.
- Jordan MA, Wilson L. Microtubules as a target for anticancer drugs. *Nat Rev Cancer.* 2004;4:253–265.
- Kasibhatla S, Baichwal V, Cai SX, et al. MPC-6827: a small-molecule inhibitor of microtubule formation that is not a substrate for multidrug resistance pumps. *Cancer Res.* 2007;67:5865–5871.
- Tsimberidou AM, Akerley W, Schabel MC, et al. Phase I clinical trial of MPC-6827 (Azixa), a microtubule destabilizing agent, in patients with advanced cancer. *Mol Cancer Ther.* 2010;9:3410–3419.
- Grossmann KF, Colman H, Akerley WA, et al. Phase I trial of verubulin (MPC-6827) plus carboplatin in patients with relapsed glioblastoma multiforme. *J Neuro-Oncol.* 2012;110:257–264.
- Chamberlain MC, Grimm S, Phuphanich S, et al. A phase 2 trial of verubulin for recurrent glioblastoma: a prospective study by the brain tumor investigational consortium (BTIC). *J Neuro-Oncol.* 2014;118:335–343.
- Gangjee A, Zhao Y, Lin Y, et al. Synthesis and discovery of water-soluble microtubule targeting agents that bind to the colchicine site on tubulin and circumvent pgp mediated resistance. *J Med Chem.* 2010;53:8116–8128.
- Combes S, Barbier P, Douillard S, et al. Synthesis and biological evaluation of 4-aryl coumarin analogues of combretastatins. part 2. *J Med Chem.* 2011;54:3153–3162.
- Cao D, Liu Y, Yan W, et al. Design, synthesis, and evaluation of *in vitro* and *in vivo* anticancer activity of 4-substituted coumarins: a novel class of potent tubulin polymerization inhibitors. *J Med Chem.* 2016;59:5721–5739.
- Plano D, Karelia DN, Pandey MK, Spallholz JE, Amin S, Sharma AK. Design, synthesis, and biological evaluation of novel selenium (Se-NSAID) molecules as anticancer agents. *J Med Chem.* 2016;59:1946–1959.
- Yan Jun, Chen J, Zhang S, Hu J, Huang L, Li X. Synthesis, evaluation, and mechanism study of novel indole-chalcone derivatives exerting effective antitumor activity through microtubule destabilization *in vitro* and *in vivo*. *J Med Chem.* 2016;59:5264–5283.
- Pang Y, An B, Lou L, et al. Design, synthesis, and biological evaluation of novel selenium-containing isocombretastatins and phenstatins as antitumor agents. *J Med Chem.* 2017;60:7300–7314.
- Bonne D, Heusele C, Simon C, Pantaloni D. 4',6-Diamidino-2-phenylindole, a fluorescent probe for tubulin and microtubules. *J Biol Chem.* 1985;260:2819–2825.
- Díaz JF, Andreu JM. Assembly of purified GDP-tubulin into microtubules induced by taxol and taxotere: reversibility, ligand stoichiometry, and competition. *Biochemistry.* 1993;32:2747–2755.
- An Baijiao, Zhang S, Yan J, Li X. Synthesis, *in vitro* and *in vivo* evaluation of new hybrids of millepachine and phenstatin as potent tubulin polymerization inhibitors. *Org Biomol Chem.* 2017;15.